J Appl Physiol 125: 1411–1423, 2018.
First published August 9, 2018; doi:10.1152/japplphysiol.01036.2017.

RESEARCH ARTICLE

Acclimatization of low altitude-bred deer mice (*Peromyscus maniculatus*) to high altitude

D. Merrill Dane,[1] Khoa Cao,[1] Hua Lu,[1] Cuneyt Yilmaz,[1] Jamie Dolan,[2] Catherine D. Thaler,[2] Priya Ravikumar,[1] Kimberly A. Hammond,[2] and Connie C. W. Hsia[1]

[1]*Department of Internal Medicine, University of Texas Southwestern Medical Center, Dallas, Texas; and* [2]*Department of Evolution, Ecology and Organismal Biology, University of California at Riverside, Riverside, California*

Submitted 20 November 2017; accepted in final form 26 July 2018

Dane DM, Cao K, Lu H, Yilmaz C, Dolan J, Thaler CD, Ravikumar P, Hammond KA, Hsia CC. Acclimatization of low altitude-bred deer mice (*Peromyscus maniculatus*) to high altitude. *J Appl Physiol* 125: 1411–1423, 2018. First published August 9, 2018; doi:10.1152/japplphysiol.01036.2017.—A colony of deer mice subspecies (*Peromyscus maniculatus sonoriensis*) native to high altitude (HA) has been maintained at sea level for 18–20 generations and remains genetically unchanged. To determine if these animals retain responsiveness to hypoxia, one group (9–11 wk old) was acclimated to HA (3,800 m) for 8 wk. Age-matched control animals were acclimated to a lower altitude (LA; 252 m). Maximal O_2 uptake ($\dot{V}O_{2max}$) was measured at the respective altitudes. On a separate day, lung volume, diffusing capacity for carbon monoxide (DL_{CO}), and pulmonary blood flow were measured under anesthesia using a rebreathing technique at two inspired O_2 tensions. The HA-acclimated deer mice maintained a normal $\dot{V}O_{2max}$ relative to LA baseline. Compared with LA control mice, antemortem lung volume was larger in HA mice in a manner dependent on alveolar O_2 tension. Systemic hematocrit, pulmonary blood flow, and standardized DL_{CO} did not differ significantly between groups. HA mice showed a higher postmortem alveolar-capillary hematocrit, larger alveolar ducts, and smaller distal conducting structures. In HA mice, absolute volumes of alveolar type I epithelia and endothelia were higher whereas that of interstitia was lower than in LA mice. These structural changes occurred without a net increase in whole-lung septal tissue-capillary volumes or surface areas. Thus, deer mice bred and raised to adulthood at LA retain phenotypic plasticity and adapt to HA without a decrement in $\dot{V}O_{2max}$ via structural (enlarged airspaces, alveolar septal remodeling) and nonstructural (lung expansion under hypoxia) mechanisms and without an increase in systemic hematocrit or compensatory lung growth.

NEW & NOTEWORTHY Deer mice (*Peromyscus maniculatus*) are robust and very active mammals that are found across the North American continent. They are also highly adaptable to extreme environments. When introduced to high altitude they retain remarkable adaptive ability to the low-oxygen environment via lung expansion and remodeling of existing lung structure, thereby maintaining normal aerobic capacity without generating more red blood cells or additional lung tissue.

aerobic capacity; high altitude; hypoxia; lung diffusing capacity; lung morphometry; ultrastructure

INTRODUCTION

Deer mice (*Peromyscus maniculatus*) are native to the North American continent at both low and high altitudes (LA and HA, respectively) from below sea level in Death Valley to over 4,300 m above sea level in the high mountains of California and Colorado (20, 63). In previous research, we have shown that when laboratory-bred adult deer mice (descended from wild HA populations) that are similar in age, health status, and developmental history are moved from LA to HA (390 m to >3,000 m) their aerobic performance at HA is initially significantly diminished (18, 55), and then it gradually recovers during an acclimation period. After 6–8 wk of acclimation, their aerobic performance recovers to levels not different from that before transport to HA and is accompanied by an increase in lung mass and volume (18, 62). When tested in normoxia, the HA-acclimated mice had a higher aerobic performance than LA mice without acclimation to HA (55). Furthermore, our previous studies show that the lung mass (18) and volume (55) of deer mice increases with acclimation to HA. Although we find the above results consistently, we have not been able to determine if the larger lung volumes after acclimation are responsible for a greater diffusion of oxygen. We speculated that the recovery of aerobic scope is due to the increase in lung mass and volume, but pulmonary oxygen uptake has not been measured in these mice before and after acclimation to HA. Here, we hypothesize that deer mice, as adults, possess significant capacity for phenotypic plasticity in pulmonary oxygen uptake during adaptation to HA. Our goal was to characterize the adaptive changes in lung structure and cardiopulmonary function in deer mice bred at LA and recently acclimated to HA and to relate these changes to aerobic performance.

A colony of a subspecies (*P. maniculatus sonoriensis*) native to the mountains of California has been maintained at the University of California Riverside (UCR; 252 m altitude) and the Peromyscus Genetic Stock Center (Columbia, SC; 98 m altitude) for 18–20 generations and has been shown to remain genetically similar (no loss of genetic variation) to the wild strain (Peromyscus Genetic Stock Center, Janet Crossland, unpublished observations). To examine how these mice, maintained at LA, adapt to HA, one group (9–11 wk old) was brought to HA (3,800 m) where they resided for 8 wk before being studied at HA (HA group). Other age-matched deer mice were maintained and studied at UCR at an LA (LA group). Maximal O_2 uptake ($\dot{V}O_{2max}$) was measured pre- and postacclimation. Lung function was measured in both groups post-

Address for reprint requests and other correspondence: C. C. W. Hsia, Univ. of Texas Southwestern Medical Center, 5323 Harry Hines Blvd., Dallas, TX 75390-9034 (e-mail: Connie.Hsia@utsouthwestern.edu).

 8750-7587/18 Copyright © 2018 the American Physiological Society

Downloaded from journals.physiology.org/journal/jappl (193.140.001.200) on February 25, 2022.

acclimation and allometrically compared with that in other adult outbred and inbred laboratory murine strains studied by the same method at the University of Texas Southwestern Medical Center (130 m altitude). Finally, alveolar septal ultrastructure was measured postmortem.

MATERIALS AND METHODS

Animals. Animal studies were carried out under protocols approved by the Institutional Animal Care and Use Committees of the University of Texas Southwestern Medical Center, the White Mountain Research Station, and UCR. A total of 26 male deer mice (*P. maniculatus sonoriensis*) were used. Animals were captive-bred at LA (252 m, UCR, CA and 88 m, Columbia, SC) from a colony established from animals caught in the White Mountains of eastern California in 1997 and 18–20 generations removed from wild deer mice. All deer mice underwent measurement of $\dot{V}O_{2max}$ at LA. Then, one group of deer mice ($n = 13$, 9–11 wk of age) was brought to HA (3,800 m) at the Barcroft Laboratory of the University of California White Mountain Research Center where they resided for 8 wk before $\dot{V}O_{2max}$ was measured at HA. Another group of age-matched male deer mice ($n = 13$) remained simultaneously at LA at UCR for 8 wk before $\dot{V}O_{2max}$ was measured again at LA. Thereafter, a subset of deer mice ($n = 10$ per group) underwent postacclimation lung function testing at their respective altitude of residence (HA or LA) 5 to 8 days after the $\dot{V}O_{2max}$ measurement.

Lung function testing used a rebreathing technique we first established in laboratory murine strains, including outbred male Swiss Webster mice (12 wk old, $n = 8$, Charles River, Wilmington, MA) and inbred C57BL/6 mice (Charles River) that were bred at sea level and studied at the University of Texas Southwestern in Dallas, TX (130 m altitude). A cohort of female 57BL/6 mice (14 to 54 wk old, $n = 9$) was used to compare measurements directly by rebreathing and single-breath maneuvers. Another cohort of male 57BL/6 mice (~18 wk old, $n = 14$) underwent rebreathing lung function testing for allometric comparisons with that in other murine strains and various other species reported in the literature, which used mostly males.

$\dot{V}O_{2max}$. $\dot{V}O_{2max}$ in deer mice was measured by open-flow respirometry during forced treadmill exercise. Air was supplied either by outlet (UCR) or using a positive pressure pump (Barcroft). Incurrent air was dried by Drierite (Xenia, OH) and scrubbed of carbon dioxide by soda lime. Flow rate was regulated by Porter mass flow controllers (Hatfield, PA) upstream of the treadmill. The working section of the treadmill was enclosed by Plexiglas (dimensions 6 × 7 × 13 cm). Flow rates of 2,300 and 1,550 ml/min [corrected to standard temperature and pressure (760 mmHg)] conditions were used at UCR and Barcroft, respectively. Approximately 150 ml/min of excurrent air was subsampled, dried, and scrubbed of CO_2 before being routed through the oxygen sensor. Oxygen concentration was analyzed with Ametek/Applied Electrochemistry S-3A analyzers (Pittsburgh, PA) and then digitized by Sable Systems UI-2 (Las Vegas, NV) A–D converters and recorded on a Macintosh computer running Warthog Laboratory Helper software (http://www.warthog.ucr.edu).

Body mass was measured before all runs. Mice were then placed on the treadmill and allowed to adjust for 2–4 min. During this time, a reference reading of unbreathed air was obtained. The treadmill was then started at a low speed (~0.1 m/s), and the speed subsequently increased by increments of 0.1 m/s every 30–45 s until the mouse could either no longer maintain position on the tread or $\dot{V}O_2$ did not increase with increasing speed. At this time, the treadmill was stopped, but $\dot{V}O_2$ measurements continued for several minutes during the animal's recovery period before a second reference reading was recorded.

$\dot{V}O_2$ was calculated from O_2 concentrations using the mode 1 equation in Warthog Laboratory Analyst software (http://www.warthog.ucr.edu)

$$\dot{V}_{O_2} = \dot{V}\frac{(F_{I_{O_2}} - F_{E_{O_2}})}{1 - F_{E_{O_2}}}$$

where $\dot{V}$ is flow rate (ml/min correcting to standard temperature and pressure), and $F_{I_{O_2}}$ and $F_{E_{O_2}}$ are incurrent (reference) and excurrent fractional O_2 concentrations, respectively ($F_{I_{O_2}}$ was assumed to be 0.2095, and $F_{E_{O_2}}$ never fell below 0.2080). An "instantaneous" correction was applied to account for mixing (5) and to resolve short-term metabolic changes better. This is a common adjustment when measuring O_2 consumption in small vertebrates and insects. Correction is necessary because in the small volume of the test chamber on the treadmill, build-up of O_2 and CO_2 can cause measurement errors. $\dot{V}O_{2max}$ was calculated as the highest 1-min average during the running bout or postexercise recovery period.

Lung function measurements. On a separate day after measurement of $\dot{V}O_{2max}$, lung function was assessed at the animal's altitude of residence ($n = 10$ per group). The animal was anesthetized by intraperitoneal injection of ketamine (50 mg/kg) and xylazine (5 mg/kg). The neck, chest, and abdomen were shaved. A longitudinal neck incision exposed the trachea, which was cannulated (20-gauge adaptor) and tied securely (3-0 silk) for mechanical ventilation (Columbus Instruments, Columbus, OH) at a respiratory rate of 150 breaths/min and tidal volume of 8 ml/kg increasing to 10–12 ml/kg as needed to maintain O_2 saturation above 90%. Heart rate and transcutaneous O_2 saturation were monitored using a tail probe (Vet/Ox G2, West Yorkshire, UK). The tracheal cannula was attached to a manifold that switched between the ventilator circuit and a small calibrated glass syringe (1 ml) for delivering precise gas volumes. Total apparatus dead space was 0.065 ml. Airway pressure was recorded using a pressure transducer (model no. 1100, Hans Rudolph, Shawnee, KS) calibrated before each experiment against a manometer. Data were acquired (100 Hz) using a laptop computer, a data acquisition card (PCM-DAS08, Computer Boards, Middleboro, MA), and LabView software (National Instruments, Austin, TX).

Airway pressure-lung volume relationship. The ventilator was paused and the lungs inflated with a known volume of air using the glass syringe. Each delivered volume was held for 6 s. Airway pressure at 3 s after the initial peak pressure was recorded, followed by expiration to air and switching back to the ventilator circuit. Volumes were delivered in 10-ml/kg increments until airway pressure reached 30 cm H_2O, then repeated in reverse order. Duplicate measurements were averaged.

Rebreathing measurements. The technique is similar as that described for rats (78). The rebreathing gas mixture consisted of 0.3% CO, 0.5% Ne, 0.8% C_2H_2, and either 40% O_2 or 90% O_2 in balance N_2. The animal breathed 25% O_2 for 2 min before each measurement using 40% O_2 and 100% O_2 for 2 min before each measurement using 90% O_2. Initial gas concentrations were measured by a gas chromatograph (Varian, Micro GC Model 4900, Santa Clara, CA) with two columns (M5AHIBF and PPUHI) and a thermal conductivity detector using 100% high-purity helium as a carrier gas. The ventilator was paused; a test gas volume equivalent to the inflation volume needed to reach 20 cmH_2O airway pressure was delivered to the lungs. Rebreathing was conducted by gently pumping the syringe at 60 strokes/min to mix the test gas with resident lung gas for 5, 7, or 9 s in separate maneuvers. The order of measurement using gas mixture containing either 40% or 90% O_2 was randomized. Precise rebreathing duration was determined from simultaneous airway pressure tracings. Mechanical ventilation resumed at the end of each rebreathing maneuver. The final syringe volume was recorded, then diluted with a known volume (0.7 to 1.0 ml) of 100% N_2 for the measurement of final gas concentrations. Dilution was necessary to ensure a sufficient sample volume for the gas chromatograph. Expired gas concentrations were calculated by considering the dilution ratios. From these measurements, disappearance curves were constructed for Ne, CO, and C_2H_2. Each maneuver was performed in duplicate, and the results were averaged. The interval between successive rebreath-

Downloaded from journals.physiology.org/journal/jappl (193.140.001.200) on February 25, 2022.

ing maneuvers was at least 2 min. At the end of rebreathing maneuvers, CO back pressure was determined by delivering 3 ml of 100% O_2 to the lungs, performing the rebreathing maneuver for 60 s, and measuring the final expired CO concentration.

Analysis of physiological data. The airway pressure-lung volume (PV) curves were analyzed using a standard approach (57). Lung volumes were calculated from Ne dilution and expressed at body temperature and pressure saturated conditions. Compliance was calculated for airway pressures between 10 and 30 cmH_2O. Pulmonary blood flow and lung diffusing capacity for carbon monoxide (DL_{CO}) were calculated from the slopes of the logarithmic disappearance curves of C_2H_2 and CO, respectively, relative to the corresponding Ne concentration during rebreathing (77). The serial components of DL_{CO}, alveolar membrane diffusing capacity (DM_{CO}), and pulmonary capillary blood volume (Vc), were calculated from measurements made at two alveolar O_2 tensions following the Roughton-Forster (RF) technique (54); these values were used to express DL_{CO} under standardized conditions ($DL_{CO\text{-}std}$) at a constant alveolar O_2 tension ($P_{A_{O_2}}$, 120 mmHg) and hematocrit (0.45) and were plotted with respect to pulmonary blood flow. The gas exchanging alveolar septal tissue volume was calculated by extrapolating the C_2H_2 disappearance curve to *time zero* (56).

Comparing rebreathing and single-breath measurements. To validate our rebreathing method in mice, female 57BL/6J mice were studied using both rebreathing and single-breath techniques. Following completion of rebreathing maneuvers as described above, the same volume of test gas mixture as in the rebreathing maneuvers was delivered to the lung; the breath was held for 10 s followed by expiration. The expired gas volume recovered in the glass syringe was measured, then diluted with 1.0 ml of 100% nitrogen, and the gas concentrations measured by gas chromatography. Lung volume was calculated from Ne dilution. DL_{CO} was calculated from the rate of CO disappearance during breath hold. Breath-hold maneuvers were performed in duplicate in each animal, and the results were averaged.

Terminal procedures. For tissue harvest, 7 LA and 6 HA deer mice were deeply anesthetized and mechanically ventilated as above. The chest cavity was opened via a midline abdominal incision. Blood was drawn from the left ventricle with a heparinized syringe for measurement of hematocrit. Pentobarbital overdose (150 mg/kg) was administered by intraperitoneal injection. The lungs were removed, fixed by tracheal instillation of 2.5% buffered glutaraldehyde at a constant airway pressure (25 cm H_2O), and immersed in 2.5% glutaraldehyde while maintaining airway pressure.

Morphometric measurements. Volume of the intact lung was measured by saline immersion (73). The lungs were serially sectioned (3-mm intervals) starting with a random orientation. Four tissue blocks were systematically sampled per animal (1 each from the upper and the lower half of each lung). Tissue blocks were postfixed with 1% osmium tetroxide in 0.1 M cacodylate buffer, treated with 2% uranyl acetate, dehydrated through graded alcohol, and embedded in Spurr (Electron Microscopy Sciences, Hartfield, PA). A 3-level stratified analytical scheme [low-power light microscopy (LM; ×275), high-power LM (×550), and transmission electron microscopy (TEM; ~×21,000)] was employed (14, 24). For low- and high-power LM, each block was sectioned (1 μm) and stained with toluidine blue. One section per block was overlaid with a test grid at the appropriate magnification. From a random start, at least 20 nonoverlapping microscopic fields per block (80 per lung) were systematically examined at ×275 magnification. Using point counting, airways or blood structures >20 μm in diameter (nonfine parenchyma) were excluded from the reference space to estimate the volume density of fine parenchyma, alveolar ducts, and sacs per unit lung volume. At ×550 magnification, 15 nonoverlapping microscopic fields per block (60 per lung) were systematically imaged from a random start. The volume density of alveolar septa per unit lung volume was estimated from the number of points falling on alveolar septa relative to the total number of points falling on fine parenchyma.

For TEM, two blocks (one from each lung) per animal were sectioned (70-nm thickness), mounted on copper grids, and examined at ~×21,000 (JEOL EXII). Thirty nonoverlapping TEM fields per grid were systematically examined (total 60 per animal). Volume densities of epithelia, interstitia, and endothelia were estimated by point counting with the alveolar septum as the reference space. Alveolar epithelial and capillary surface densities per unit septum volume were estimated by intersection counting. At least 300 points or intersections were counted per grid. The volume and surface densities at each level were related through the cascade of levels to the total lung volume to obtain absolute volumes (ml) and surface areas (cm^2). The lengths of test lines that transect the tissue-plasma barrier (from air-epithelial interface to the nearest erythrocyte membrane) were measured to estimate the harmonic mean thickness of the tissue-plasma barrier, an anatomical index of resistance of the blood-gas barrier to diffusion. Enough samples, blocks, and fields were examined to reduce the coefficients of variation in the major parameters of volume and surface densities and harmonic mean thickness of the tissue-plasma barrier to ≤10%.

Statistical analysis. Because of significant differential changes in body mass between groups during acclimation, we show the results (mean ± SD) in both absolute and body mass-specific values. Changes in body mass and $\dot{V}O_{2max}$ were compared by paired *t*-test and analysis of covariance. Lung function data were compared between groups using factorial ANOVA or unpaired *t*-test. Correlation between DL_{CO} and pulmonary blood flow was evaluated by linear regression analysis; slopes and intercepts were compared between groups by the method of Zar (80). Differences at $P \leq 0.05$ were considered significant.

RESULTS

Physiological measurements in deer mice. Baseline body mass at LA was not different between groups (Table 1). After acclimation, body mass increased in LA deer mice (+12.5% from baseline, $P = 0.03$) but changed minimally in HA deer mice (+3% from baseline) and became significantly lower than that in LA mice ($P = 0.02$). As the animals were fed the same diet, the findings likely reflect a lower activity level and/or higher food intake in the LA group. Baseline absolute $\dot{V}O_{2max}$ at our LA site was borderline (8%) lower in deer mice that subsequently acclimated to HA ($P = 0.06$). Following acclimation, mean absolute $\dot{V}O_{2max}$ increased 7% in HA mice and declined 2% in LA mice. Postacclimation absolute $\dot{V}O_{2max}$ was not significantly different between HA and LA deer mice (Table 1; Fig. 1). The change in $\dot{V}O_{2max}$ (post/pre ratio) (HA 1.08 ± 0.16, LA 0.99 ± 0.08, mean ± SD) was not signifi-

Table 1. $\dot{V}O_{2max}$

Exposure	LA	HA	*P* Value
Number of animals	13	13	
Preacclimation			
Body mass, g	20.8 ± 2.8	19.0 ± 3.4	0.18
$\dot{V}O_{2max}$, ml/min	4.52 ± 0.47	4.15 ± 0.48	0.06#
$\dot{V}O_{2max}$, ml·(min·kg)$^{-1}$	220 ± 24	222 ± 31	0.84
Postacclimation			
Body mass, g	23.3 ± 4.5[a]	19.6 ± 2.75	0.02*
$\dot{V}O_{2max}$, ml/min	4.43 ± 0.40	4.46 ± 0.73	0.94*
$\dot{V}O_{2max}$, ml·(min·kg)$^{-1}$	195 ± 31[a]	228 ± 28	0.008*
Post-/preacclimation $\dot{V}O_{2max}$ ratio	0.99 ± 0.08	1.08 ± 0.16	0.08

Values are mean ± SD. HA, high altitude; LA, low altitude; $\dot{V}O_{2max}$, maximal O_2 uptake. Body mass was measured on each day of study. *$P \leq 0.05$; #$P = 0.06$: HA vs. LA, unpaired *t*-test; [a]$P < 0.002$: post- vs. preacclimation, paired *t*-test.

Downloaded from journals.physiology.org/journal/jappl (193.140.001.200) on February 25, 2022.

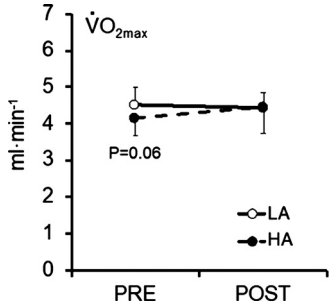


Fig. 1. $\dot{V}O_{2max}$ in deer mice was measured at low altitude (LA) preacclimation and at either low (LA) or high altitude (HA) postacclimation ($n = 13$ animals each). Preacclimation absolute $\dot{V}O_{2max}$ was lower in the HA than the LA group at a borderline significance ($P = 0.06$). Postacclimation $\dot{V}O_{2max}$ was not significantly different between groups. Mean ± SD. $\dot{V}O_{2max}$, maximal O_2 uptake.

cantly different ($P = 0.08$) but may be biologically meaningful.

Systemic hematocrit and lung function were measured 5–8 days following the postacclimation $\dot{V}O_{2max}$ measurement ($n = 10$ deer mice per group, Table 2). Systemic hematocrit was not different between HA and LA deer mice. Lung volume at a given airway pressure was significantly higher in HA deer mice than LA deer mice (Fig. 2). Specific compliance of the respiratory system was not significantly different between HA and LA groups (Table 2).

A representative set of expiratory gas concentrations obtained during rebreathing maneuvers in one animal is shown in Fig. 3. Complete mixing of the test gas bolus with resident alveolar gas was achieved rapidly during rebreathing; Ne concentration stabilized within 5 s whereas C_2H_2 and CO concentrations declined in a log linear fashion with time, similar as that observed in rats (78, 79), guinea pigs (76), and larger species. As expected at the respective altitudes of study, mean $P_{A_{O_2}}$ during rebreathing was lower in the HA than in the LA group (Table 2). Mean CO back pressure was negligible (LA: 0.0016%, HA: 0.0008%).

While rebreathing the 40% O_2 mixture (mean $P_{A_{O_2}}$ of 214 and 125 mmHg, LA and HA, respectively), lung volume and DL_{CO} were significantly higher in the HA group; pulmonary blood flow also tended to be higher but reached statistical significance only when normalized by body mass (Table 2).

While rebreathing the 90% O_2 mixture (mean Pa_{O_2} 469 and 292 mmHg, LA and HA, respectively), none of the absolute measurements were statistically different between groups; however, body mass-specific lung volumes were significantly higher in the HA group (Table 2). The derived values of DM_{CO}, Vc, $DL_{CO\text{-}std}$, and alveolar septal tissue were not significantly different between groups (Table 2) except that body mass-specific $DL_{CO\text{-}std}$ was higher in HA animals ($P = 0.03$). Average absolute DL_{CO} at a given pulmonary blood flow was not significantly different between HA and LA groups (Fig. 4).

Compare rebreathing and single-breath measurements in laboratory mice. Mean end-inspiratory lung volume and DL_{CO} measured by the rebreathing technique agreed closely with that measured by the single-breath technique (Fig. 5).

Allometry. Mean lung volume, DL_{CO}, and pulmonary blood flow measured by the rebreathing technique in deer mice and outbred and inbred laboratory mice fit well with the respective allometric relationships across a wide range of species assembled from the literature (Fig. 6); these represent measurements obtained by single-breath, steady state, or rebreathing techniques at rest either under anesthesia (4, 8–11, 13, 17, 19, 23, 26, 29, 31, 33, 34, 36, 38, 43–45, 47, 48, 51, 52, 58, 65, 68, 70, 72, 74) or during conscious spontaneous breathing (1, 3, 12, 25, 39, 42, 53, 77).

Morphometric measurements in deer mice. Postmortem lung fixation was performed in seven and six deer mice at LA and HA, respectively. Terminal body weight was 11% lower and absolute volume of the fixed lungs was 7% higher in HA mice; neither difference was significant ($P = 0.14$ and 0.32, respectively). However, body mass-specific lung volume was significantly (34%) higher in HA mice ($P = 0.02$, Table 3). Morphometric alveolar-capillary hematocrit measured by point counting was 23% higher, in contrast to the similar antemortem systemic hematocrit (Table 2). The arithmetic and harmonic mean septal thicknesses were similar between groups (Table 3). Volume density of fine parenchyma (per unit of lung volume) was significantly higher whereas volume density of nonfine parenchyma was lower in HA than LA deer mice ($P < 0.001$, Table 4). Volume density of alveolar ducts, but not alveolar sacs, was higher in the HA group (Fig. 7). Volume densities of type I epithelia were 37% higher and type II epithelia 32% lower in HA deer mice; thus, overall volume density of epithelia was unchanged. Volume density of interstitia was significantly (20%) lower in HA-acclimated deer mice whereas that of endothelia was not different between groups. Total volume densities of septum, septal tissue, capillary blood, and alveolar and capillary surface densities (surface area/lung volume ratios) were not different between groups (Table 4).

In HA-acclimated deer mice, absolute volume of nonfine parenchyma was 50% lower than that in LA mice ($P = 0.004$) whereas that of fine parenchyma was borderline higher (15%, $P = 0.07$). Absolute volumes of the alveolar duct, type I epithelia, and endothelia were significantly higher (by 47%, 48%, and 28%, respectively) in HA deer mice than that in LA deer mice, whereas the volume of interstitia was 15% lower ($P = 0.05$), and the volume of type II epithelia was nonsignificantly lower ($P = 0.08$). (Table 5, Fig. 8). Total volume of the septum, extravascular septal tissue, or alveolar-capillary blood was not significantly different between groups. Total alveolar and capillary surface areas were not different between groups (Table 5). These results are consistent with acinar airway enlargement, reduced dimensions of small bronchioles, arterioles and venules, and volume shifts among alveolar septal constituents in HA-acclimated deer mice.

DISCUSSION

Summary of findings. These are the first detailed examinations of lung function and ultrastructure in a subspecies of deer mice native to HA. Our goal was to determine the adaptive response in deer mice bred at LA and recently acclimated to HA and to relate lung architecture to cardiopulmonary function and aerobic performance. To accomplish this goal, deer mice captive-bred at LA for 18–20 generations were acclimated as adults to HA (3,800 m) for 8 wk whereas matched control deer mice were acclimated to LA (252 m). To assess alveolar-capillary function, we validated a rebreathing technique to

Downloaded from journals.physiology.org/journal/jappl (193.140.001.200) on February 25, 2022.

Table 2. *Lung function*

Exposure	LA	HA	*P* Value
Number of animals	10	10	
Terminal body mass, g	22.5 ± 4.1	18.8 ± 3.3	0.02*
Systemic hematocrit, %	42.3 ± 2.4	44.2 ± 3.6	0.27
Respiratory system compliance§, ml·(cmH_2O)$^{-1}$	0.021 ± 0.005	0.020 ± 0.006	0.69
Specific respiratory system compliance§, ml·(cmH_2O·ml)$^{-1}$	0.067 ± 0.027	0.051 ± 0.016	0.08
Rebreathing Mixture Containing 40% O_2:			
Mean alveolar P_{O_2} (40% O_2), mmHg	214 ± 31	125 ± 13	<0.0001*
Expiratory lung volume			
ml	0.35 ± 0.09	0.47 ± 0.08	0.003*
ml/kg	16.0 ± 4.7	25.8 ± 7.0	0.003*
Inspiratory lung volume			
ml	1.04 ± 0.16	1.21 ± 0.17	0.03*
ml/kg	47.2 ± 10.0	66.2 ± 16.9	0.002*
Pulmonary blood flow			
ml/min	3.31 ± 1.15	4.41 ± 2.35	0.19
ml·(min·kg)$^{-1}$	142 ± 47	242 ± 150	0.03*
$DL_{CO\text{-}measured}$			
ml·(min·mmHg)$^{-1}$	0.0097 ± 0.0034	0.0136 ± 0.0042	0.05*
ml·(min·mmHg·kg)$^{-1}$	0.43 ± 0.13	0.74 ± 0.26	0.001*
Septal tissue volume			
ml	0.30 ± 0.21	0.20 ± 0.06	0.26
ml/kg	12.9 ± 8.5	10.4 ± 2.5	0.41
Rebreathing Mixture Containing 90% O_2:			
Mean alveolar P_{O_2} (90% O_2), mmHg	469 ± 62	292 ± 30	<0.0001*
Expiratory lung volume			
ml	0.36 ± 0.12	0.41 ± 0.06	0.21
ml/kg	15.7 ± 5.8	22.1 ± 4.8	0.006*
Inspiratory lung volume			
ml	1.05 ± 0.20	1.14 ± 0.15	0.20
ml/kg	46.6 ± 11.0	62.5 ± 14.6	0.005*
Pulmonary blood flow			
ml/min	3.72 ± 1.20	3.72 ± 1.37	0.99
ml·(min·kg)$^{-1}$	164 ± 57	193 ± 53	0.30
$DL_{CO\text{-}measured}$			
ml·(min·mmHg)$^{-1}$	0.0063 ± 0.0025	0.0067 ± 0.0023	0.73
ml·(min·mmHg·kg)$^{-1}$	0.27 ± 0.11	0.36 ± 0.09	0.11
Septal tissue volume			
ml	0.18 ± 0.11	0.16 ± 0.07	0.91
ml/kg	7.6 ± 4.7	8.3 ± 3.2	0.84
Derived from the Roughton-Forster Model:			
DM_{CO}			
ml·(min·mmHg)$^{-1}$	0.0255 ± 0.0106	0.0228 ± 0.0111	0.73
ml·(min·mmHg·kg)$^{-1}$	1.16 ± 0.43	1.23 ± 0.61	0.82
Pulmonary capillary blood volume			
ml	0.0293 ± 0.0099	0.0569 ± 0.0278	0.47
ml/kg	1.34 ± 0.43	2.88 ± 1.30	0.13
$DL_{CO\text{-}std}$			
ml·(min·mmHg)$^{-1}$	0.0093 ± 0.0024	0.0114 ± 0.0036	0.24
ml·(min·mmHg·kg)$^{-1}$	0.43 ± 0.11	0.60 ± 0.14	0.03*

Body mass was measured on the day of study. Mean ± SD. DL_{CO}, lung diffusing capacity for carbon monoxide; DM_{CO}, membrane diffusing capacity for carbon monoxide; $DL_{CO\text{-}measured}$, measured DL_{CO}; $DL_{CO\text{-}std}$, standardized DL_{CO} (hematocrit 0.45, alveolar P_{O_2} 120 mmHg). *$P \leq 0.05$: HA versus LA, unpaired *t*-test or one-way ANOVA. §Respiratory system compliance was measured at airway pressures between 10 and 30 cm H_2O.

measure lung volume, pulmonary blood flow, and diffusion simultaneously in mice at their respective altitude of residence. Major findings are: *1*) deer mice maintained their body mass and $\dot{V}_{O_{2max}}$ at HA relative to LA baseline; *2*) HA deer mice did not exhibit an increase in systemic hematocrit that is typical of lowland species acclimatized to HA. However, postmortem anatomical alveolar capillary hematocrit was significantly higher; *3*) HA deer mice exhibited a 40% larger static lung volume at a given airway pressure in ambient hypoxia and higher lung volumes and DL_{CO} measured while rebreathing a 40% O_2 gas mixture but not while rebreathing a 90% O_2 mixture. Specific respiratory system compliance was similar; *4*) the relationships of absolute $DL_{CO\text{-}std}$, DM_{CO}, and Vc with respect to pulmonary blood flow were not significantly different between groups; *5*) postmortem body mass-specific lung volume but not absolute lung volume was larger in HA-acclimated deer mice. Alveolar ducts were enlarged whereas the volumes of small airways and microvessels were smaller without significant differences in whole-lung volumes of extravascular septal tissue, capillary blood, or alveolar-capillary surface areas, compared with LA-acclimated deer mice, i.e., there was no compensatory lung growth in HA mice; *6*) HA-acclimated mice exhibited alveolar septal remodeling with higher volumes of alveolar type I epithelia and endothelia, and

Downloaded from journals.physiology.org/journal/jappl (193.140.001.200) on February 25, 2022.

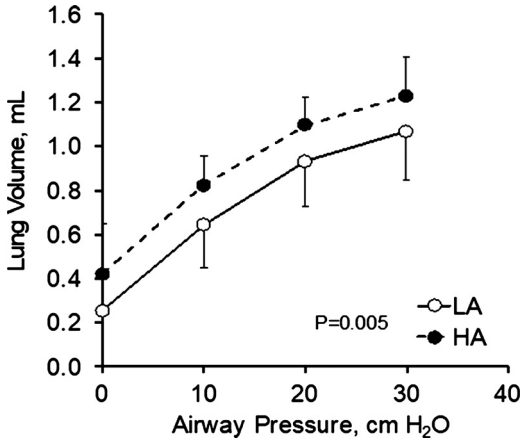


Fig. 2. Static airway pressure-lung volume relationships during lung inflation by ambient air showed a significantly larger lung volume in HA-acclimated than LA-acclimated deer mice (10 animals each). Mean ± SD. $P = 0.005$ HA vs. LA, by repeated measures ANOVA.

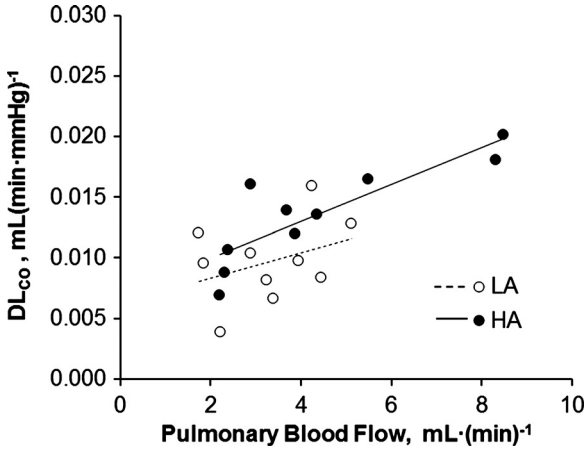


Fig. 4. Relationship between average DL_{CO} and pulmonary blood flow in individual animals measured while rebreathing an inspired gas mixture containing 40% O_2. At a given blood flow, DL_{CO} was not significantly different between HA and LA deer mice by analysis of the slopes and elevations of regression lines ($P = 0.97$ and $P = 0.61$, respectively). DL_{CO}, lung diffusing capacity for carbon monoxide; HA, high altitude; LA, low altitude.

a lower volume of interstitia, without any change in harmonic mean barrier thickness, an index of blood-gas barrier resistance to diffusion. Thus, deer mice bred and raised to adulthood at LA adapt very well to subsequent HA residence via nonstructural ($P_{A_{O_2}}$-dependent increase in lung volume) and structural (distal airspace enlargement and septal remodeling) adjustments such that there is no significant decrement in cardiopulmonary O_2 transport or aerobic capacity at HA compared with control animals kept at an LA.

Critique of methodology. Body mass and $\dot{V}_{O_{2max}}$ in our deer mice were in a similar range as that reported previously (18). Using deer mice that have been vivarium-bred at sea level ensures consistent genetic background, age, sex, and living condition among individual animals and avoids the risks of exposing research personnel to Hanta virus that is carried by wild deer mice and is responsible for the lethal human Hantavirus pulmonary syndrome. To ensure that results reflect actual physiological response, baseline measurements were performed at the LA whereas postacclimation measurements were performed at each animal's place of residence (HA or LA). DL_{CO} was expressed at standardized $P_{A_{O_2}}$ and hematocrit following established methodology. Separate laboratory murine strains were also studied to compare measurements obtained using the rebreathing technique with that using a single-breath technique and to establish that rebreathing measurements fit with the respective allometric relationships among murine strains and across multiple species over a wide range of body sizes. Key morphometric results fall within the body mass-specific range as that previously reported in the literature in laboratory mice (32, 37, 69, 71).

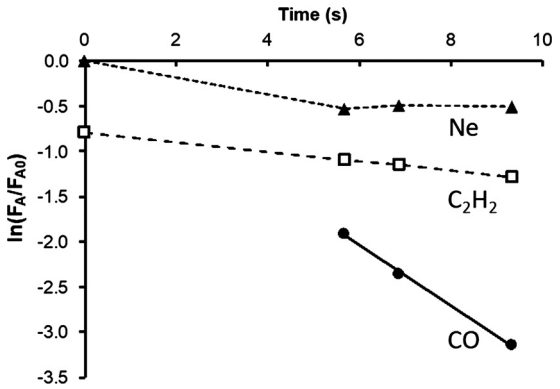


Fig. 3. A representative set of logarithmic expiratory gas concentration curves for neon (Ne), acetylene (C_2H_2), and carbon monoxide (CO) obtained during rebreathing maneuvers in one mouse. F_A, fractional alveolar gas concentration; F_{A0}, initial fractional alveolar gas concentration (at *time zero*).

Physiological adaptation to HA in the lungs of deer mice. Wild deer mice remain active throughout the year in the extreme HA habitat where they must overcome ambient hypoxia, cold temperatures, and food scarcity. They have evolved novel hemoglobin isoforms with increased O_2 binding affinity to surmount partially the low ambient O_2 availability (7, 27, 64); however, these isoforms are not always expressed and are insufficient to support the aerobic demands of deer mice fully, necessitating other strategies to increase O_2 uptake and delivery. Hammond et al. (18) reported that deer mice that were raised and tested at LA exhibit higher aerobic capacity and basal metabolic rate than those that were either raised or acclimated as adults and tested at HA. Aerobic performance at HA is similar between HA-raised deer mice and LA-raised mice acclimated to HA as adults. These results suggest that in addition to genetic and developmental factors, postnatal acclimatization plays an important role in deer mice adaption to HA. Consistent with the present findings, Shirkey and Hammond (62) observed that $\dot{V}_{O_{2max}}$ of deer mice on arrival at HA is lower than it is after acclimation, indicating adaptation. In our deer mice, body mass was maintained following HA-acclimation but increased significantly in the LA control group. As the animals were fed the same diet, the findings likely reflect lower activity level and/or higher food intake in the LA group. Hammond et al. (50) also demonstrated larger lung volume and heart mass in deer mice acclimated to hypoxia that correlated with aerobic performance, suggesting that increased cardiopulmonary O_2 transport capacities helped HA-acclimated deer mice adapt to ambient hypoxia.

Direct comparisons of postacclimation lung volumes and DL_{CO} between the HA and LA groups were complicated by a large difference in $P_{A_{O_2}}$ at the two altitudes of measurement. In

Downloaded from journals.physiology.org/journal/jappl (193.140.001.200) on February 25, 2022.

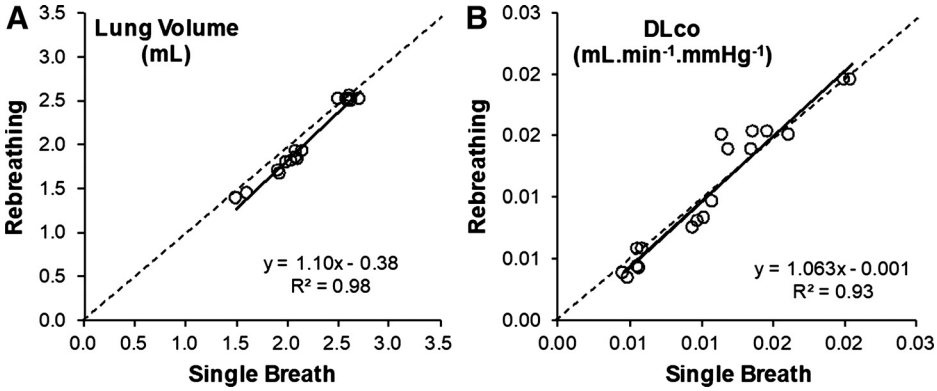


Fig. 5. Correlations between measurements using a rebreathing or a single-breath technique for end-inspiratory lung volume (*A*) and DL_{CO} (*B*) in C57BL/6 mice (9 animals, 2 measurements per animal). Solid line: linear regression. Dashed line: identity. DL_{CO}, lung diffusing capacity for carbon monoxide.

deer mice acclimatized to and studied at HA, static PV relationship while breathing ambient air was clearly elevated; lung volume was significantly higher when measured while rebreathing a 40% O_2 mixture (mean $P_{A_{O_2}}$ 125 mmHg) but not while rebreathing a 90% O_2 mixture (mean $P_{A_{O_2}}$ 292 mmHg). The differential findings may reflect an acute physiological response to changes in $P_{A_{O_2}}$. Both acute and chronic hypoxia induce adaptation in neural ventilatory drive and lung mechanics. In human subjects, acute reductions in $P_{A_{O_2}}$ increase total lung capacity, end-expiratory lung volume, residual volume, and static expiratory lung compliance; the effect is thought to be mediated by a loss of smooth muscle tone in distal airways that mildly reduces lung elastic recoil and airway resistance (59) and by a reduction in total pulmonary blood volume because of pulmonary vasoconstriction (41).

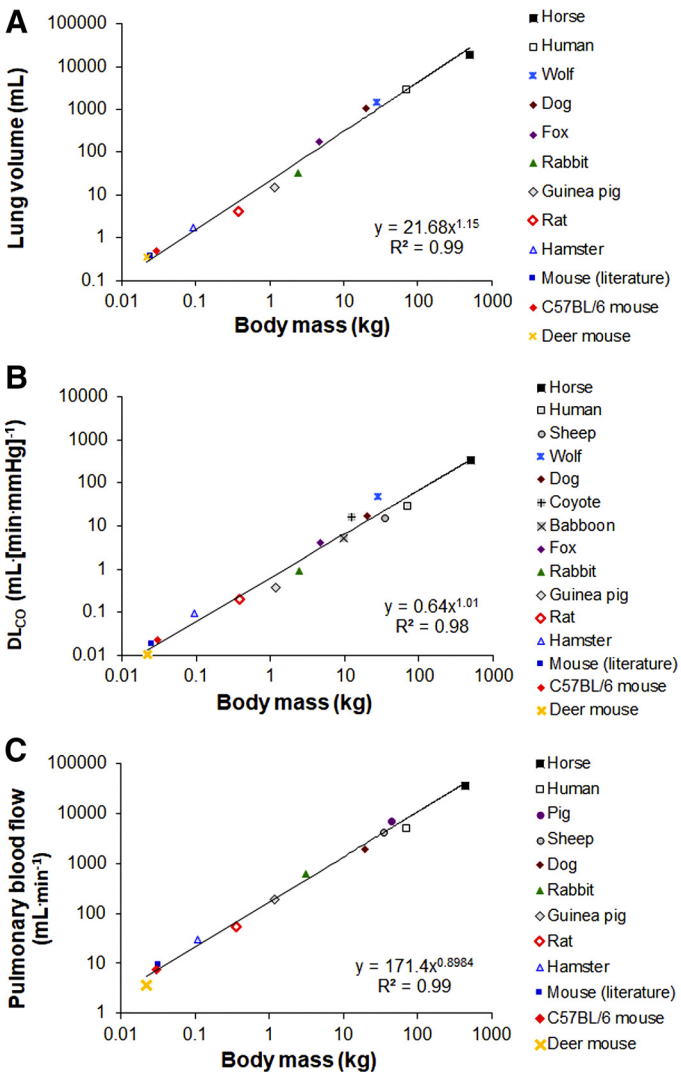


Fig. 6. Allometric relationships for mean lung volume (*A*), DL_{CO} (*B*), and pulmonary blood flow (*C*) in males of different species reported in the literature. Data on the following murine strains are from the present study: male C57BL/6, and male LA-acclimated deer mice. See text for references to the other source data. DL_{CO}, lung diffusing capacity for carbon monoxide; LA, low altitude.

Our usual technique for standardizing DL_{CO} is to calculate DM_{CO} and Vc using the RF model, then use the derived DM_{CO} and Vc to express DL_{CO} at constant conditions ($DL_{CO\text{-}std}$, at $P_{A_{O_2}}$ 120 mmHg, hematocrit 45%). When this was done, $DL_{CO\text{-}std}$ in HA mice was modestly (23%) though nonsignificantly higher. Others have reported modest increases in DL_{CO} in human lowlanders acclimatized to HA; Agostoni et al. (2) found a 6% higher adjusted DL_{CO} measured at rest following 2 wk acclimation to 5,400 m altitude. Taylor et al. (67) observed a 10% higher resting DL_{CO} following ~6 wk acclimation at up to 5,150 m altitude. In our HA-acclimated mice, the lack of significant differences in $DL_{CO\text{-}std}$, DM_{CO}, and Vc is internally consistent with postmortem data showing nondifference in whole-lung alveolar tissue-capillary volumes, surface areas, and barrier thickness compared with LA-acclimated mice.

Because O_2 and CO compete for the same binding sites on hemoglobin, at a constant inspired O_2 concentration the lower O_2 tension at HA results in an increase in DL_{CO} of ~0.35% for each mmHg of reduction in $P_{A_{O_2}}$. To verify the nonsignificantly higher $DL_{CO\text{-}std}$ observed in HA mice further, we empirically adjusted the measured DL_{CO} ($DL_{CO\text{-}measured}$) to a constant $P_{A_{O_2}}$ (120 mmHg) without using DM_{CO} and Vc: $DL_{CO\text{-}altitude\ adjusted} = DL_{CO\text{-}measured} \times [1.0 + 0.0035 \cdot (P_{A_{O_2}} - 120)]$. This adjustment indeed confirms a nonsignificantly higher (9%) altitude-adjusted DL_{CO} in HA mice (LA: 0.0127 ± 0.0037, HA: 0.0138 ± 0.0043 ml·(min·mmHg)$^{-1}$, $P = 0.52$). Thus, the higher DL_{CO} in HA mice measured while rebreathing at a mean $P_{A_{O_2}}$ of 125 mmHg (but not 292 mmHg) is likely the result of both the physical effect of hypobaric hypoxia and an acute P_{O_2}-dependent increase in lung volume.

Sources of variability in DL_{CO}, DM_{CO}, and Vc should also be noted. There is inherent imprecision in the dilution of a small, expired sample volume. The RF model assumes DM_{CO}

Downloaded from journals.physiology.org/journal/jappl (193.140.001.200) on February 25, 2022.

Table 3. *Morphometric measurements*

Exposure	LA	HA	*P* Value
Number of animals	7	6	
Terminal body mass, g	21.4 ± 1.91	19.1 ± 3.26	0.14
Total lung volume, immersion method			
ml	0.74 ± 0.08	0.79 ± 0.12	0.32
ml/kg	31.3 ± 5.12	41.8 ± 3.53	0.02*
Morphometric hematocrit, %	58.2 ± 7.2	71.7 ± 6.6	0.01*
Mean arithmetic thickness of septum, μm	1.86 ± 0.31	1.82 ± 0.16	0.79
Mean arithmetic thickness of septal tissue, μm	0.87 ± 0.09	0.84 ± 0.79	0.52
Mean harmonic thickness of blood-gas barrier, μm	0.39 ± 0.05	0.38 ± 0.04	0.53

Values are means ± SD. HA, high altitude, LA, low altitude. *$P \leq 0.05$: HA versus LA, unpaired *t*-test.

and Vc to be serial independent parameters. However, finite element modeling of alveolar-capillary diffusion (21) has shown intrinsic interdependence between DM_{CO} and Vc, i.e., increasing Vc recruits capillaries and effective membrane surface for diffusion, thereby increasing DM_{CO}. The RF model further assumes that DM_{CO} and Vc are independent of $P_{A_{O_2}}$ whereas finite element modeling has shown a decrease in effective DM_{CO} as $P_{A_{O_2}}$ increases (22). Errors arising from model assumptions are normally minor for small variations in $P_{A_{O_2}}$ but may be magnified across a large range of $P_{A_{O_2}}$ as in this study, a fact that likely accentuated the variability of derived DM_{CO} and Vc values.

Structural adaptation to HA in the lungs of deer mice. In contrast to the elevated PV relationship in HA deer mice breathing ambient air (Fig. 2), postmortem absolute volume of the fixed lung was not significantly different between groups. As the animals received supplemental O_2 during the terminal procedure, this finding is consistent with a $P_{A_{O_2}}$-dependent change in antemortem lung volume described above. However, body mass-specific lung volume was significant higher in HA animals. There was preferential enlargement of alveolar ducts as has been reported in other species exposed to chronic hypoxia (79) whereas distal conducting structures were smaller such that there were no net gains in whole-lung alveolar septal tissue or capillary volumes or gas exchange surface areas in HA-acclimated deer mice. The lack of whole-lung compensatory tissue-capillary growth or a change in harmonic mean barrier thickness is consistent with the absence of significant differences in $DL_{CO\text{-}std}$, DM_{CO}, and Vc between HA and LA deer mice and is consistent with that in HA-acclimated adult canines (30, 31). Findings in adult animals contrast with that in young, growing animals where HA residence or chronic hypoxia exposure before reaching somatic maturity leads to lung volume enlargement and accelerated gains in alveolar-capillary tissue volumes and surface areas (6, 30, 31, 75). In addition to enlarged acinar airways, HA deer mice showed clear evidence of alveolar septal remodeling, including modest shifts in volume densities and absolute volumes of septal constituents toward more type I and less type II epithelia without a change in total epithelia volume and more endothelia with less interstitia to minimize diffusive resistance of the blood-gas barrier and to help prevent a decrement in $\dot{V}O_{2max}$ at HA.

Table 4. *Volume and surface densities of alveolar septal structures*

Volume Density of Alveolar Structure, per unit lung volume			
Exposure	LA	HA	*P* Value
Fine parenchyma	0.87764 ± 0.02534	0.94244 ± 0.02621	0.0009*
Nonfine parenchyma	0.12237 ± 0.02534	0.05757 ± 0.02621	0.0009*
Alveolar ducts	0.27760 ± 0.0203	0.33106 ± 0.02736	0.002*
Alveoli	0.50219 ± 0.02502	0.51920 ± 0.02393	0.24
Septum	0.08706 ± 0.0069	0.08219 ± 0.00953	0.31
Total epithelium	0.01752 ± 0.0021	0.01869 ± 0.00201	0.33
Type I epithelium	0.00971 ± 0.00115	0.01334 ± 0.00116	0.0001*
Type II epithelium	0.00782 ± 0.0016	0.00536 ± 0.0021	0.04*
Interstitium	0.03917 ± 0.0026	0.03153 ± 0.00669	0.02*
Endothelium	0.00841 ± 0.00181	0.00999 ± 0.00161	0.13
Septal tissue	0.0651 ± 0.00387	0.06021 ± 0.00764	0.16
Capillary blood	0.02196 ± 0.00482	0.02199 ± 0.00475	0.99
Surface Density of Alveolar Structure, per unit lung volume/cm			
Alveolar surface	955.66 ± 138.81	906.28 ± 83.88	0.46
Capillary surface	548.04 ± 71.79	523.77 ± 62.22	0.53

Values are means ± SD. HA, high altitude; LA, low altitude. *$P \leq 0.05$: HA versus LA, unpaired *t*-test.

Systemic hematocrit was similar in our HA- and LA-acclimatized deer mice. In contrast, Hammond et al. (18) reported significantly higher systemic hematocrits and hemoglobin concentrations in LA-raised deer mice acclimatized to the same HA (3,800 m) over 3 wk compared with LA-raised/LA-acclimated deer mice. These divergent findings may be related to differences in the duration of HA exposure or the timing and manner of blood sampling; in the earlier study by Hammond et al. (18) blood was drawn via retro-orbital puncture shortly after the animal exercised to $\dot{V}O_{2max}$ on the treadmill whereas in the present study blood was drawn via cardiac puncture under anesthesia. Despite a similar systemic hematocrit, postmortem alveolar-capillary hematocrit measured by point-counting was higher in HA-acclimated deer mice, suggesting relatively greater erythrocyte sequestration within alveolar microvasculature. The difference between systemic and morphometric hematocrit partly reflects trapping of erythrocytes as pulmonary microvascular blood flow ceases following the overdose of euthanasia solution. Because systemic hematocrit was not different between HA and LA groups, a higher morphometric hematocrit also suggests higher pulmonary microvascular outflow resistance, perhaps a result of hypoxic pulmonary microvascular reactivity (16), in the HA group.

Other adaptations in O_2 transport. In our anesthetized HA-acclimated deer mice, body mass-specific pulmonary blood flow was higher than in LA-acclimated animals; the difference may become accentuated when awake and active. The skeletal muscle of native highland deer mice populations exhibit a higher respiratory capacity via more oxidative fibers containing a higher volume density of subsarcolemmal mitochondria situated closer to capillaries (61). Upon acclimation

Downloaded from journals.physiology.org/journal/jappl (193.140.001.200) on February 25, 2022.

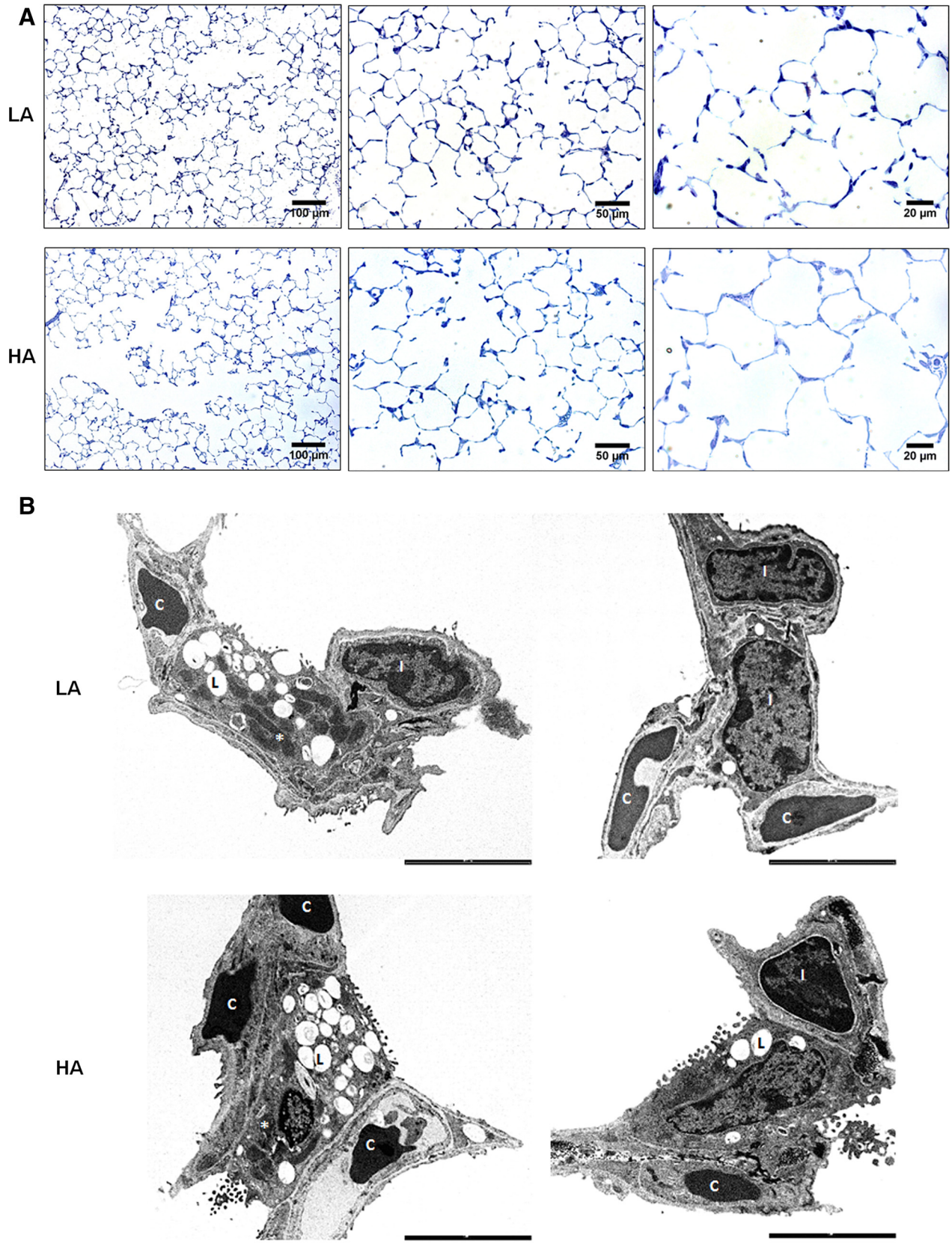


Fig. 7. Representative microscopic images in deer mice acclimated to low (LA) or high (HA) altitude. *Top*: light micrographs of distal lung morphology. Toluidine blue stain (bar = 100, 50, 20 μm, left to right). *Bottom*: electron micrographs of alveolar septal morphology (bar = 5 μm). Symbol indicates a representative feature: *Mitochondria within a type II epithelial cell. C, capillary erythrocyte; I, interstitial cell; L, lamellar body.

Downloaded from journals.physiology.org/journal/jappl (193.140.001.200) on February 25, 2022.

Table 5. *Absolute volumes and surface areas of septal structures*

	LA	HA	*P* Value
	Absolute Volume, mm^3		
Fine parenchyma			
mm^3	647.176 ± 68.986	746.795 ± 110.114	0.07
ml/kg	30.500 ± 4.231	39.291 ± 2.487	0.001*
Nonfine parenchyma			
mm^3	90.253 ± 21.353	46.038 ± 23.230	0.004*
ml/kg	4.294 ± 1.312	2.464 ± 1.341	0.030*
Alveolar ducts			
mm^3	179.414 ± 20.873	263.184 ± 49.582	0.002*
ml/kg	8.435 ± 1.039	13.798 ± 1.311	0.000005*
Alveoli			
mm^3	396.379 ± 50.495	411.514 ± 62.272	0.64
ml/kg	18.706 ± 3.090	21.661 ± 1.797	0.06
Septum			
mm^3	64.061 ± 6.989	64.356 ± 5.437	0.93
ml/kg	3.018 ± 0.406	3.423 ± 0.391	0.095
Total epithelium			
mm^3	12.904 ± 1.868	14.725 ± 2.049	0.12
ml/kg	0.612 ± 0.129	0.779 ± 0.088	0.022*
Type I epithelium			
mm^3	7.119 ± 0.763	10.558 ± 1.752	0.0006*
ml/kg	0.337 ± 0.056	0.554 ± 0.035	0.00001*
Type II epithelium			
mm^3	5.785 ± 1.421	4.167 ± 1.630	0.08
ml/kg	0.275 ± 0.082	0.224 ± 0.089	0.31
Interstitium			
mm^3	28.783 ± 2.359	24.609 ± 4.458	0.05*
ml/kg	1.357 ± 0.171	1.302 ± 0.212	0.62
Endothelium			
mm^3	6.146 ±1.160	7.845 ± 1.333	0.03*
ml/kg	0.288 ± 0.052	0.417 ± 0.072	0.003*
Septal tissue			
mm^3	47.833 ± 3.589	47.179 ± 5.266	0.8
ml/kg	2.257 ± 0.294	2.498 ± 0.223	0.13
Capillary blood			
mm^3	16.228 ± 4.115	17.177 ± 3.442	0.66
ml/kg	0.760 ± 0.173	0.925 ± 0.243	0.18
	Absolute Surface Area, cm^2		
Alveolar surface			
cm^2	704 ± 123	715 ± 106	0.86
m^2/kg	3.332 ± 0.738	3.773 ± 0.335	0.21
Capillary surface			
cm^2	404 ± 65	411 ± 45	0.83
m^2/kg	1.899 ± 0.319	2.19 ± 0.335	0.14

Values are means ± SD. HA, high altitude; LA, low altitude. *$P \leq 0.05$: HA versus LA, unpaired *t*-test.

to hypoxia, native highland deer mice exhibit higher diaphragmatic respiratory capacity via increased capillary density (66) and mitochondrial quantity (35) whereas native lowlanders exhibit additional increases in citrate synthase activity and release of reactive O_2 species (35). These peripheral adjustments augment O_2 unloading and tissue diffusion-utilization, counterbalancing the effects of a higher hemoglobin-O_2 affinity that promotes O_2 loading in the lung (28).

Comparison among murine strains. The arithmetic alveolar septal thickness in LA-acclimated deer mice (1.86 μm) is considerably lower than that in Sv129 mice measured under electron microscopy (3.48 μm, Hsia laboratory, unpublished observations) and CD1 (2.4 μm) (60) and C57/BL6 (~3.4 μm) (69) mice measured under light microscopy whereas the arithmetic thickness of septal tissue barrier in deer mice (0.87 μm) is lower than that in white (1.25 μm) and Japanese Waltzing (1.08 μm) mice (15); differences are at least partly because of a higher alveolar surface area relative to septum volume in deer mice, which facilitates diffusive O_2 uptake. In contrast to the lack of HA-stimulated lung growth in deer mice, Darwin's leaf-eared mice (*Phyllotis darwini*) living at HA show enlarged alveolar septal cell volumes and mass-specific surface areas compared with the same species living at sea level (46). Laboratory (C57BL/6) mice also exhibit accelerated lung growth during chronic intermittent hypoxia (49). As the generation of new lung tissue requires higher metabolic energy expenditure than remodeling of existing lung tissue, deer mice are far more efficient at defending O_2 transport via both inborn and hypoxia-induced adaptations.

Conclusion and significance. We assessed aerobic capacity and lung structure and function in deer mice (*P. maniculatus sonoriensis*) that have been bred for many generations and raised to adulthood at LA and subsequently acclimated to HA to determine how these animals accommodate their native HA habitat. We found that these deer mice remain well adapted to HA, exhibiting no decrement in $\dot{V}O_{2max}$ at HA and only modest structural alterations following acclimation. The major adaptive mechanisms during acclimation are alveolar O_2 tension-dependent increases in lung volume, distal airspace enlarge-

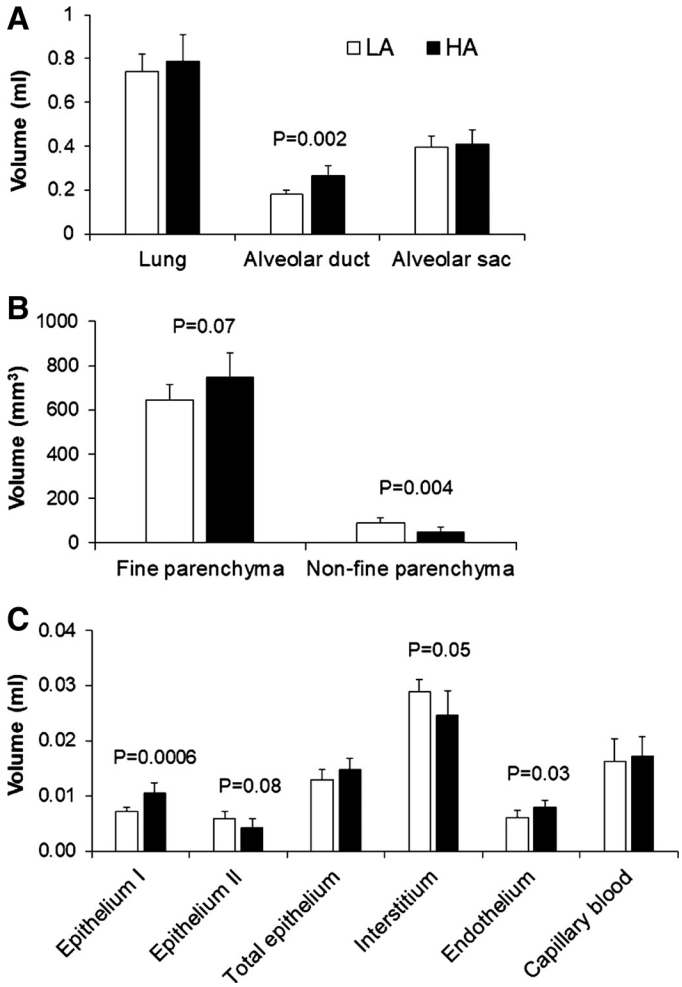


Fig. 8. Postmortem absolute volumes of the lung, alveolar ducts and alveolar sacs (*A*), fine and nonfine parenchyma (*B*), and alveolar septal constituents (*C*) in deer mice acclimatized to high (HA) or low (LA) altitude (n = 6 and 7 animals, respectively). Mean ± SD. Significant *P* values by unpaired *t*-test are shown.

Downloaded from journals.physiology.org/journal/jappl (193.140.001.200) on February 25, 2022.

ment, and alveolar septal remodeling; these changes occur without systemic polycythemia or active alveolar tissue-capillary growth and are sufficient to maintain pulmonary diffusive O_2 uptake and a normal aerobic capacity to meet the demands for survival in a harsh environment. Beyond these structure-function relationships, our study has ecological implications. Over the last century, more than half of the 28 small mammalian species measured across a 3,000-m altitude gradient in Yosemite National Park in California (~100 miles to the west of our study site at White Mountain) have moved up in elevation where daily minimum temperatures are cooler (40). This is consistent with an observed 3°C increase in daily minimum temperatures over the same period. Further increases in minimum temperatures in this region are predicted, which will continue to alter the species migration pattern and the predator/prey relationships at mid to high elevations. Understanding the phenotypic plasticity and species-specific parameters of adaptation will be critical in predicting future distribution and welfare of deer mice populations at HAs.

ACKNOWLEDGMENTS

The authors thank the staff of the Animal Resource Center at University of Texas (UT) Southwestern and University of California at Riverside for veterinary care, and the Electron Microscopy Core Facility at UT Southwestern for technical assistance.

GRANTS

This work was supported by the National Science Foundation Grant No. 145700 (to K. Hammond) and the National Heart, Lung and Blood Institute Grant Nos. U01-HL-111146 and R01-HL-134373 from the National Institutes of Health (both to C. Hsia).

DISCLAIMERS

The content is solely the authors' responsibility and does not necessarily represent official views of the funding agencies.

DISCLOSURES

No conflicts of interest, financial or otherwise, are declared by the authors.

AUTHOR CONTRIBUTIONS

K.A.H. and C.C.W.H. conceived and designed research; D.M.D., K.C., H.L., C.Y., J.D., C.D.T., P.R., K.A.H., and C.C.W.H. performed experiments; D.M.D., K.C., H.L., C.Y., J.D., C.D.T., K.A.H., and C.C.W.H. analyzed data; D.M.D., K.C., C.D.T., K.A.H., and C.C.W.H. interpreted results of experiments; D.M.D., K.C., and C.C.W.H. prepared figures; D.M.D., K.C., and C.C.W.H. drafted manuscript; K.A.H. and C.C.W.H. edited and revised manuscript; D.M.D., K.C., C.D.T., K.A.H., and C.C.W.H. approved final version of manuscript.

REFERENCES

1. **Adaro F, Meyer M, Sikand RS.** Rebreathing and single breath pulmonary CO diffusing capacity in man at rest and exercise studied by C18O isotope. *Bull Eur Physiopathol Respir* 12: 747–756, 1976.
2. **Agostoni P, Swenson ER, Bussotti M, Revera M, Meriggi P, Faini A, Lombardi C, Bilo G, Giuliano A, Bonacina D, Modesti PA, Mancia G, Parati G; HIGHCARE Investigators.** High-altitude exposure of three weeks duration increases lung diffusing capacity in humans. *J Appl Physiol (1985)* 110: 1564–1571, 2011. doi:10.1152/japplphysiol.01167.2010.
3. **Aguilera-Tejéro E, Pascoe JR, Amis TC, Kurpershoek CJ, Woliner MJ.** Measurement of pulmonary diffusing capacity for carbon monoxide and functional residual capacity during rebreathing in conscious thoroughbreds. *Am J Vet Res* 54: 1752–1757, 1993.
4. **Baker DG, Lin YC.** Local thermodilution: a reliable technique for estimating renal blood flow in the rabbit. *Comp Biochem Physiol A* 72: 157–160, 1982. doi:10.1016/0300-9629(82)90025-1.
5. **Bartholomew GA, Vleck D, Vleck CM.** Instantaneous measurements of oxygen consumption during pre-flight warm-up and post-flight cooling in sphingid and saturniid moths. *J Exp Biol* 90: 17–32, 1981.
6. **Burri PH, Weibel ER.** Morphometric estimation of pulmonary diffusion capacity. II. Effect of Po2 on the growing lung, adaption of the growing rat lung to hypoxia and hyperoxia. *Respir Physiol* 11: 247–264, 1971. doi:10.1016/0034-5687(71)90028-4.
7. **Chappell MA, Hayes JP, Snyder LRG.** Hemoglobin polymorphisms in deer mice (Peromyscus maniculatus): physiology of beta-globin variants and alpha-globin recombinants. *Evolution* 42: 681–688, 1988. doi:10.1111/j.1558-5646.1988.tb02486.x.
8. **Chen L, Zhang J, Gan TX, Chen-Izu Y, Hasday JD, Karmazyn M, Balke CW, Scharf SM.** Left ventricular dysfunction and associated cellular injury in rats exposed to chronic intermittent hypoxia. *J Appl Physiol (1985)* 104: 218–223, 2008. doi:10.1152/japplphysiol.00301.2007.
9. **Collins JF, McCullough B, Coalson JJ, Johanson WG JR.** Bleomycin-induced diffuse interstitial pulmonary fibrosis in baboons. II. Further studies on connective tissue changes. *Am Rev Respir Dis* 123: 305–312, 1981. doi:10.1164/arrd.1981.123.3.305.
10. **Costa DL, Kutzman RS, Lehmann JR, Drew RT.** Altered lung function and structure in the rat after subchronic exposure to acrolein. *Am Rev Respir Dis* 133: 286–291, 1986. doi:10.1164/arrd.1986.133.2.286.
11. **Crapo JD, Crapo RO.** Comparison of total lung diffusion capacity and the membrane component of diffusion capacity as determined by physiologic and morphometric techniques. *Respir Physiol* 51: 183–194, 1983. doi:10.1016/0034-5687(83)90039-7.
12. **Crapo RO, Crapo JD, Morris AH.** Lung tissue and capillary blood volumes by rebreathing and morphometric techniques. *Respir Physiol* 49: 175–186, 1982. doi:10.1016/0034-5687(82)90072-X.
13. **de los Santos R, Coalson JJ, Holcomb JR, Johanson WG JR.** Hyperoxia exposure in mechanically ventilated primates with and without previous lung injury. *Exp Lung Res* 9: 255–275, 1985. doi:10.3109/01902148509057527.
14. **Foster DJ, Ravikumar P, Bellotto DJ, Unger RH, Hsia CC.** Fatty diabetic lung: altered alveolar structure and surfactant protein expression. *Am J Physiol Lung Cell Mol Physiol* 298: L392–L403, 2010. doi:10.1152/ajplung.00041.2009.
15. **Geelhaar A, Weibel ER.** Morphometric estimation of pulmonary diffusion capacity. 3. The effect of increased oxygen consumption in Japanese Waltzing mice. *Respir Physiol* 11: 354–366, 1971. doi:10.1016/0034-5687(71)90009-0.
16. **Grover RF, Johnson RL JR, McCullough RG, McCullough RE, Hofmeister SE, Campbell WB, Reynolds RC.** Pulmonary hypertension and pulmonary vascular reactivity in beagles at high altitude. *J Appl Physiol (1985)* 65: 2632–2640, 1988. doi:10.1152/jappl.1988.65.6.2632.
17. **Hallowell GD, Corley KT.** Use of lithium dilution and pulse contour analysis cardiac output determination in anaesthetized horses: a clinical evaluation. *Vet Anaesth Analg* 32: 201–211, 2005. doi:10.1111/j.1467-2995.2005.00249.x.
18. **Hammond KA, Chappell MA, Kristan DM.** Developmental plasticity in aerobic performance in deer mice (Peromyscus maniculatus). *Comp Biochem Physiol A Mol Integr Physiol* 133: 213–224, 2002. doi:10.1016/S1095-6433(02)00159-9.
19. **Harris RS, Hadian M, Hess DR, Chang Y, Venegas JG.** Pulmonary artery occlusion increases the ratio of diffusing capacity for nitric oxide to carbon monoxide in prone sheep. *Chest* 126: 559–565, 2004. doi:10.1378/chest.126.2.559.
20. **Hock RJ.** Physiological responses of deer mice to various native altitudes. In: *Physiological Effects of High Altitude*, edited by Weihe WH. London: Pergamon Press, 1964, p. 59–72. doi:10.1016/B978-1-4831-6699-5.50013-9
21. **Hsia CC, Chuong CJ, Johnson RL JR.** Critique of conceptual basis of diffusing capacity estimates: a finite element analysis. *J Appl Physiol (1985)* 79: 1039–1047, 1995. doi:10.1152/jappl.1995.79.3.1039.
22. **Hsia CC, Chuong CJ, Johnson RL JR.** Red cell distortion and conceptual basis of diffusing capacity estimates: finite element analysis. *J Appl Physiol (1985)* 83: 1397–1404, 1997. doi:10.1152/jappl.1997.83.4.1397.
23. **Hsia CC, Herazo LF, Ramanathan M, Johnson RL JR.** Cardiopulmonary adaptations to pneumonectomy in dogs. IV. Membrane diffusing capacity and capillary blood volume. *J Appl Physiol (1985)* 77: 998–1005, 1994. doi:10.1152/jappl.1994.77.2.998.
24. **Hsia CC, Hyde DM, Ochs M, Weibel ER; ATS/ERS Joint Task Force on Quantitative Assessment of Lung Structure.** An official research

Downloaded from journals.physiology.org/journal/jappl (193.140.001.200) on February 25, 2022.

policy statement of the American Thoracic Society/European Respiratory Society: standards for quantitative assessment of lung structure. *Am J Respir Crit Care Med* 181: 394–418, 2010. doi:10.1164/rccm.200809-1522ST.

25. **Hsia CC, McBrayer DG, Ramanathan M.** Reference values of pulmonary diffusing capacity during exercise by a rebreathing technique. *Am J Respir Crit Care Med* 152: 658–665, 1995. doi:10.1164/ajrccm.152.2.7633723.
26. **Hsia CC, Yan X, Dane DM, Johnson RL JR.** Density-dependent reduction of nitric oxide diffusing capacity after pneumonectomy. *J Appl Physiol (1985)* 94: 1926–1932, 2003. doi:10.1152/japplphysiol.00525.2002.
27. **Inoguchi N, Mizuno N, Baba S, Kumasaka T, Natarajan C, Storz JF, Moriyama H.** Alteration of the α1β2/α2β1 subunit interface contributes to the increased hemoglobin-oxygen affinity of high-altitude deer mice. *PLoS One* 12: e0174921, 2017. doi:10.1371/journal.pone.0174921.
28. **Jensen B, Storz JF, Fago A.** Bohr effect and temperature sensitivity of hemoglobins from highland and lowland deer mice. *Comp Biochem Physiol A Mol Integr Physiol* 195: 10–14, 2016. doi:10.1016/j.cbpa.2016.01.018.
29. **Johanson WG JR, Pierce AK.** Lung structure and function with age in normal rats and rats with papain emphysema. *J Clin Invest* 52: 2921–2927, 1973. doi:10.1172/JCI107488.
30. **Johnson RL JR.** Adventures in gas exchange. In *The Pulmonary Circulation and Gas Exchange*, edited by Wagner WW Jr, Weir EK. Armonk, NY: Futura, 1994, p. 221–234.
31. **Johnson RL JR, Cassidy SS, Grover RF, Schutte JE, Epstein RH.** Functional capacities of lungs and thorax in beagles after prolonged residence at 3,100 m. *J Appl Physiol (1985)* 59: 1773–1782, 1985. doi:10.1152/jappl.1985.59.6.1773.
32. **Knudsen L, Ochs M, Mackay R, Townsend P, Deb R, Mühlfeld C, Richter J, Gilbert F, Hawgood S, Reid K, Clark H.** Truncated recombinant human SP-D attenuates emphysema and type II cell changes in SP-D deficient mice. *Respir Res* 8: 70, 2007. doi:10.1186/1465-9921-8-70.
33. **Krivitski NM, Starostin D, Smith TL.** Extracorporeal recording of mouse hemodynamic parameters by ultrasound velocity dilution. *ASAIO J* 45: 32–36, 1999. doi:10.1097/00002480-199901000-00008.
34. **Lai YL, Olson JW, Gillespie MN.** Ventilatory dysfunction precedes pulmonary vascular changes in monocrotaline-treated rats. *J Appl Physiol (1985)* 70: 561–566, 1991. doi:10.1152/jappl.1991.70.2.561.
35. **Mahalingam S, McClelland GB, Scott GR.** Evolved changes in the intracellular distribution and physiology of muscle mitochondria in high-altitude native deer mice. *J Physiol* 595: 4785–4801, 2017. doi:10.1113/JP274130.
36. **McNeil JS, Torrington KG, Mundie TG, Banks RA, Phillips YY, Ripple GR.** Prediction of carbon monoxide diffusing capacity of the lung in splenectomized sheep. *Lab Anim Sci* 41: 63–65, 1991.
37. **Meban C.** Thickness of the air-blood barriers in vertebrate lungs. *J Anat* 131: 299–307, 1980.
38. **Meyer M, Schuster KD, Schulz H, Mohr M, Piiper J.** Pulmonary diffusing capacities for nitric oxide and carbon monoxide determined by rebreathing in dogs. *J Appl Physiol (1985)* 68: 2344–2357, 1990. doi:10.1152/jappl.1990.68.6.2344.
39. **Miller JM, Johnson RL JR.** Effect of lung inflation on pulmonary diffusing capacity at rest and exercise. *J Clin Invest* 45: 493–500, 1966. doi:10.1172/JCI105363.
40. **Moritz C, Patton JL, Conroy CJ, Parra JL, White GC, Beissinger SR.** Impact of a century of climate change on small-mammal communities in Yosemite National Park, USA. *Science* 322: 261–264, 2008. doi:10.1126/science.1163428.
41. **Nelin LD, Rickaby DA, Linehan JH, Dawson CA.** The vascular site of action of hypoxia in the neonatal pig lung. *Pediatr Res* 35: 25–29, 1994. doi:10.1203/00006450-199401000-00007.
42. **Niranjan V, McBrayer DG, Ramirez LC, Raskin P, Hsia CCW.** Glycemic control and cardiopulmonary function in patients with insulin-dependent diabetes mellitus. *Am J Med* 103: 504–513, 1997. doi:10.1016/S0002-9343(97)00251-9.
43. **Okere IC, Chess DJ, McElfresh TA, Johnson J, Rennison J, Ernsberger P, Hoit BD, Chandler MP, Stanley WC.** High-fat diet prevents cardiac hypertrophy and improves contractile function in the hypertensive dahl salt-sensitive rat. *Clin Exp Pharmacol Physiol* 32: 825–831, 2005. doi:10.1111/j.1440-1681.2005.04272.x.
44. **Pauluhn J.** Repeated pulmonary function measurements in rats after intratracheal instillation of a polyamine textile pigment component. *Inhal Toxicol* 12: 591–604, 2000. doi:10.1080/08958370050030967.
45. **Pauluhn J, Baumann M, Hirth-Dietrich C, Rosenbruch M.** Rat model of lung fibrosis: comparison of functional, biochemical, and histopathological changes 4 months after single irradiation of the right hemithorax. *Toxicology* 161: 153–163, 2001. doi:10.1016/S0300-483X(00)00413-3.
46. **Pearson OP, Pearson A.** A stereological analysis of the ultrastructure of the lungs of wild mice living at low and high altitude. *J Morphol* 150: 359–368, 1976. doi:10.1002/jmor.1051500208.
47. **Raub JA, Mercer RR, Miller FJ, Graham JA, O'Neil JJ.** Dose response of elastase-induced emphysema in hamsters. *Am Rev Respir Dis* 125: 432–435, 1982. doi:10.1164/arrd.1982.125.4.432.
48. **Reinhard C, Eder G, Fuchs H, Ziesenis A, Heyder J, Schulz H.** Inbred strain variation in lung function. *Mamm Genome* 13: 429–437, 2002. doi:10.1007/s00335-002-3005-6.
49. **Reinke C, Bevans-Fonti S, Grigoryev DN, Drager LF, Myers AC, Wise RA, Schwartz AR, Mitzner W, Polotsky VY.** Chronic intermittent hypoxia induces lung growth in adult mice. *Am J Physiol Lung Cell Mol Physiol* 300: L266–L273, 2011. doi:10.1152/ajplung.00239.2010.
50. **Rezende EL, Hammond KA, Chappell MA.** Cold acclimation in Peromyscus: individual variation and sex effects in maximum and daily metabolism, organ mass and body composition. *J Exp Biol* 212: 2795–2802, 2009. doi:10.1242/jeb.032789.
51. **Richard JC, Janier M, Decailliot F, Le Bars D, Lavenne F, Berthier V, Lionnet M, Cinotti L, Annat G, Guérin C.** Comparison of PET with radioactive microspheres to assess pulmonary blood flow. *J Nucl Med* 43: 1063–1071, 2002.
52. **Rivers RJ, Beckman JB, Frame MD.** Technique for using video microscopy and indicator dilution for repeated measurements of cardiac output in small animals. *Anesthesiology* 94: 489–495, 2001. doi:10.1097/00000542-200103000-00021.
53. **Rose GL, Cassidy SS, Johnson RL JR.** Diffusing capacity at different lung volumes during breath holding and rebreathing. *J Appl Physiol Respir Environ Exerc Physiol* 47: 32–36, 1979. doi:10.1152/jappl.1979.47.1.32.
54. **Roughton FJ, Forster RE.** Relative importance of diffusion and chemical reaction rates in determining rate of exchange of gases in the human lung, with special reference to true diffusing capacity of pulmonary membrane and volume of blood in the lung capillaries. *J Appl Physiol* 11: 290–302, 1957. doi:10.1152/jappl.1957.11.2.290.
55. **Russell GA, Rezende EL, Hammond KA.** Development partly determines the aerobic performance of adult deer mice, Peromyscus maniculatus. *J Exp Biol* 211: 35–41, 2008. doi:10.1242/jeb.012658.
56. **Sackner MA, Greeneltch D, Heiman MS, Epstein S, Atkins N.** Diffusing capacity, membrane diffusing capacity, capillary blood volume, pulmonary tissue volume, and cardiac output measured by a rebreathing technique. *Am Rev Respir Dis* 111: 157–165, 1975. doi:10.1164/arrd.1975.111.2.157.
57. **Salazar E, Knowles JH.** An analysis of pressure-volume characteristics of the lungs. *J Appl Physiol* 19: 97–104, 1964. doi:10.1152/jappl.1964.19.1.97.
58. **Sardella GL, Ou LC.** Chronically instrumented rat model for hemodynamic studies of both pulmonary and systemic circulations. *J Appl Physiol (1985)* 74: 849–852, 1993. doi:10.1152/jappl.1993.74.2.849.
59. **Saunders NA, Betts MF, Pengelly LD, Rebuck AS.** Changes in lung mechanics induced by acute isocapnic hypoxia. *J Appl Physiol Respir Environ Exerc Physiol* 42: 413–419, 1977. doi:10.1152/jappl.1977.42.3.413.
60. **Schneider JP, Arkenau M, Knudsen L, Wedekind D, Ochs M.** Lung remodeling in aging surfactant protein D deficient mice. *Ann Anat* 211: 158–175, 2017. doi:10.1016/j.aanat.2017.01.013.
61. **Scott GR, Guo KH, Dawson NJ.** The mitochondrial basis for adaptive variation in aerobic performance in high-altitude deer mice. *Integr Comp Biol*: 58: 506–518, 2018. doi:10.1093/icb/icy056.
62. **Shirkey NJ, Hammond KA.** The relationship between cardiopulmonary size and aerobic performance in adult deer mice at high altitude. *J Exp Biol* 217: 3758–3764, 2014. doi:10.1242/jeb.103713.
63. **Snyder LR, Born S, Lechner AJ.** Blood oxygen affinity in high- and low-altitude populations of the deer mouse. *Respir Physiol* 48: 89–105, 1982. doi:10.1016/0034-5687(82)90052-4.

Downloaded from journals.physiology.org/journal/jappl (193.140.001.200) on February 25, 2022.

64. **Storz JF, Runck AM, Moriyama H, Weber RE, Fago A.** Genetic differences in hemoglobin function between highland and lowland deer mice. *J Exp Biol* 213: 2565–2574, 2010. doi:10.1242/jeb.042598.
65. **Takezawa J, Miller FJ, O'Neil JJ.** Single-breath diffusing capacity and lung volumes in small laboratory mammals. *J Appl Physiol Respir Environ Exerc Physiol* 48: 1052–1059, 1980. doi:10.1152/jappl.1980.48.6.1052.
66. **Tate KB, Ivy CM, Velotta JP, Storz JF, McClelland GB, Cheviron ZA, Scott GR.** Circulatory mechanisms underlying adaptive increases in thermogenic capacity in high-altitude deer mice. *J Exp Biol* 220: 3616–3620, 2017. doi:10.1242/jeb.164491.
67. **Taylor BJ, Coffman KE, Summerfield DT, Issa AN, Kasak AJ, Johnson BD.** Pulmonary capillary reserve and exercise capacity at high altitude in healthy humans. *Eur J Appl Physiol* 116: 427–437, 2016. doi:10.1007/s00421-015-3299-1.
68. **Turek Z, Grandtner M, Ringnalda BE, Kreuzer F.** Hypoxic pulmonary steady-state diffusing capacity for CO and cardiac output in rats born at a simulated altitude of 3500m. *Pflugers Arch* 340: 11–18, 1973. doi:10.1007/BF00592193.
69. **Voswinckel R, Motejl V, Fehrenbach A, Wegmann M, Mehling T, Fehrenbach H, Seeger W.** Characterisation of post-pneumonectomy lung growth in adult mice. *Eur Respir J* 24: 524–532, 2004. doi:10.1183/09031936.04.10004904.
70. **Wegner CD, Wolyniec WW, LaPlante AM, Marschman K, Lubbe K, Haynes N, Rothlein R, Letts LG.** Intercellular adhesion molecule-1 contributes to pulmonary oxygen toxicity in mice: role of leukocytes revised. *Lung* 170: 267–279, 1992. doi:10.1007/BF00566679.
71. **Weibel ER.** Morphometric estimation of pulmonary diffusion capacity. V. Comparative morphometry of alveolar lungs. *Respir Physiol* 14: 26–43, 1972. doi:10.1016/0034-5687(72)90015-1.
72. **Weibel ER, Taylor CR, O'Neil JJ, Leith DE, Gehr P, Hoppeler H, Langman V, Baudinette RV.** Maximal oxygen consumption and pulmonary diffusing capacity: a direct comparison of physiologic and morphometric measurements in canids. *Respir Physiol* 54: 173–188, 1983. doi:10.1016/0034-5687(83)90055-5.
73. **Yan X, Polo Carbayo JJ, Weibel ER, Hsia CC.** Variation of lung volume after fixation when measured by immersion or Cavalieri method. *Am J Physiol Lung Cell Mol Physiol* 284: L242–L245, 2003. doi:10.1152/ajplung.00184.2002.
74. **Yang XP, Sabbah HN, Liu YH, Sharov VG, Mascha EJ, Alwan I, Carretero OA.** Ventriculographic evaluation in three rat models of cardiac dysfunction. *Am J Physiol Heart Circ Physiol* 265: H1946–H1952, 1993. doi:10.1152/ajpheart.1993.265.6.H1946.
75. **Yilmaz C, Dane DM, Hsia CC.** Alveolar diffusion-perfusion interactions during high-altitude residence in guinea pigs. *J Appl Physiol (1985)* 102: 2179–2185, 2007. doi:10.1152/japplphysiol.00059.2007.
76. **Yilmaz C, Dane DM, Hsia CC.** Assessing recruitment of lung diffusing capacity in exercising guinea pigs with a rebreathing technique. *J Appl Physiol (1985)* 105: 316–321, 2008. doi:10.1152/japplphysiol.00155.2008.
77. **Yilmaz C, Johnson RL JR, Hsia CC.** A rebreathing method for measuring lung volume, diffusing capacity and cardiac output in conscious small animals. *Respir Physiol Neurobiol* 146: 215–223, 2005. doi:10.1016/j.resp.2004.12.010.
78. **Yilmaz C, Ravikumar P, Bellotto DJ, Unger RH, Hsia CC.** Fatty diabetic lung: functional impairment in a model of metabolic syndrome. *J Appl Physiol (1985)* 109: 1913–1919, 2010. doi:10.1152/japplphysiol.00549.2010.
79. **Yilmaz C, Ravikumar P, Gyawali D, Iyer R, Unger RH, Hsia CC.** Alveolar-capillary adaptation to chronic hypoxia in the fatty lung. *Acta Physiol (Oxf)* 213: 933–946, 2015. doi:10.1111/apha.12419.
80. **Zar JH.** *Biostatistical Analysis* (5th ed.). Englewood Cliffs, NJ: Prentice-Hall, 2009.



Downloaded from journals.physiology.org/journal/jappl (193.140.001.200) on February 25, 2022.